Toward Ultrathin Gold Nanoshells: Exploring Seed Density, Polymer Additives and Microwave Radiation Effects

Laurent Lermusiaux
Université de Bordeaux, CNRS, ICMCB, UMR 5026
Marie Plissonneau
Solvay R&I
Laure Bertry
Solvay R&I
Glenna L. Drisko
Université de Bordeaux, CNRS, ICMCB, UMR 5026
Valérie Buissette
Solvay R&I
Thierry Le Mercier
Solvay R&I
Etienne Duguet
Université de Bordeaux, CNRS, ICMCB, UMR 5026
Mona Tréguer-Delapierre (mona.treguer@icmcb.cnrs.fr)
Université de Bordeaux, CNRS, ICMCB, UMR 5026

Research Article

Keywords: Plasmonic Core-shell, Ultrathin shell, Silica particles, Seed-mediated growth, Gold

Posted Date: May 20th, 2021

DOI: https://doi.org/10.21203/rs.3.rs-524498/v1

Toward ultrathin gold nanoshells: exploring seed density, polymer additives and microwave radiation effects

Laurent Lermusiaux[1,], Marie Plissonneau[2], Laure Bertry[2], Glenna L. Drisko[1], Valérie Buissette[2], Thierry Le Mercier[2], Etienne Duguet[1], and Mona Tréguer-Delapierre[1,*]*

[1]Université de Bordeaux, CNRS, ICMCB, UMR 5026, Pessac 33600, France

[2]Solvay R&I, 52 rue de la Haie Coq, 93306, Aubervilliers, France

KEYWORDS. Plasmonic Core-shell, Ultrathin shell, Silica particles, Seed-mediated growth, Gold

ABSTRACT. Nanoshells made of a silica core and a gold shell possess an optical response that is sensitive to nanometre-scale variations in shell thickness. The exponential red shift of the plasmon resonance with decreasing shell thickness makes ultrathin nanoshells (less than 10 nm) particularly interesting for broad and tuneable ranges of optical properties. Nanoshells are generally synthesised by coating gold onto seed-covered silica particles, producing continuous shells with a lower limit of 15 nm, as a result of an inhomogeneous droplet formation on the silica surface during the seed regrowth. In this paper, we investigate the effects of three variations of the synthesis protocol to favour ultrathin nanoshells: seed density, polymer

additives and microwave treatment. We first maximised gold seed density around the silica core but surprisingly its effect is limited. However, we found that the addition of polyvinylpyrrolidone during the shell synthesis leads to higher homogeneity and a thinner shell and that a post-synthetic thermal treatment using microwaves can further smooth the particle surface. This study brings new insights into the synthesis of metallic nanoshells, pushing the limits of ultrathin shell synthesis.

INTRODUCTION

Metallic nanoshells (or core@shell particles) are nanoparticles made of a dielectric core surrounded by a metallic coating. They have attracted much attention over the past two decades because of their intense optical properties. Independent control over two parameters, *i.e.* the core radius and shell thickness, offers good tunability over the absorption and scattering cross-sections of the particles in the visible and near-infrared region. Therefore, they have been used for many applications such as water desalination and purification, as well as sterilisation,[1] fluorescence enhancement of dye molecules,[2] improvement of dye-functionalised solar cell,[3] and biosensing.[4] In general, the optical extinction of metallic nanoshells red shifts as shell thickness decreases and is located mostly in the near-infrared region for thicknesses below 10 nm, making particles with ultrathin shells of particular interest for biomedical applications in the near-infrared window.[5,6]

The synthesis of gold nanoshells was first described by Oldenburg *et al*. in three steps: surface amination of silica cores, deposition of Duff's seeds (2-3 nm gold seed) and regrowth of the seeds using a gold plating solution and a reducing agent.[7] The latter is preferentially formaldehyde because it favours a homogeneous seed growth as compared to sodium borohydride or hydroxylamine hydrochloride,[8] and because it is more practical than gaseous

CO.[9,10] In terms of the synthesis mechanism, growing seeds eventually touch and merge to form a shell. Previous experiments have shown a qualitative relationship between the seed density and the shell thickness: an increase in seed density produces thinner shells.[10,11] However, a quantitative description of this relationship is not straightforward. The formation of a continuous shell results not only from gold plating, but also from an additional process involving seeds coalescing into a smaller number of particles on the surface in the form of droplets.[12] This leads to a commonly observed intermediate state (between particles decorated with seeds and a continuous nanoshells) for which particles have a raspberry-like shape[7,8,13] and whose optical properties are well described by numerical simulations.[12] After regrowth, the synthesis eventually yields continuous shells having at least 15 nm of thickness.[2] Unfortunately, only by getting a thinner continuous shell can the red shifted extinction spectra be obtained.

Since the first report of nanoshells,[7] many variations to the protocol have been proposed to improve or accelerate the synthesis. The most common modifications include adapting the functionalising agent, the reducing agent and the reaction conditions.[11,14–18] It appears that many parameters have direct effects on the synthesis products, such as smoothness, homogeneity and continuity of the metallic shell, yet few enable the synthesis of an ultrathin continuous shell. For example, the quality of the metallic shell is dependent on the age of the seed solution[19,20] and the gold plating solution[21], the pH[22] of the latter, as well as the stirring speed during the formation of the shell.[13] On the other hand, ultrathin shells were obtained by specific parameters combination such as high seed density and $CO_{(g)}$ as reducing agent.[10] Overall, because of the high sensitivity of nanoshell synthesis to numerous parameters, to study the effects of a given parameter, it is primordial to synthesise reference samples under the same reaction conditions.

In this paper, we produce nanoshells using a seeded-growth process and vary three independent parameters to study how they improve the synthesis of ultrathin shells: seed density, polymer additives and microwave treatment. We first demonstrate that, surprisingly, maximising gold seed density on silica particles does not help to produce ultrathin shells. The seed density on the silica particles was altered by increasing ionic strength during the seed deposition and performing a second functionalisation/deposition step. Although the change in seed density significantly impacts the optical spectra before shell growth, after growth, the spectra are virtually identical. We then study adding a polymer during shell growth to favour the formation of a thin shell. Finally, we study flash microwave radiation treatment as a post-synthetic tool to smooth the nanoshells. Compared to the reference samples, these two innovative approaches led to thinner and smoother shells and exhibited an increased intensity in the extinction spectra in the near infrared.

RESULTS AND DISCUSSION

Seed-covered silica particles

In order to study the effect of seed density on the synthesis of ultrathin gold nanoshells, we synthesised nanoshells using silica particles covered with different seed densities. We used and combined two different approaches to vary and maximise the seed density on the silica particles. Because the nanoshell synthesis is highly sensitive to different experimental conditions, the different samples were prepared in parallel, to minimise the effect of environmental parameters. We first pre-synthesised highly monodisperse (polydispersity index less than 2%), ultra-smooth 300 nm silica spheres using a step-by-step growth.[24] Monodispersity improves the ensemble optical properties.[25] After functionalising the silica particles with amine groups by surface

condensation of (3-aminopropyl)trimethoxysilane (APTMS), we mixed them with 14-day old seeds under different conditions (Figure 1a). First, half were mixed without NaCl and half at a salt concentration of 60 mM of NaCl (samples A_1 and B_1 in Figure 1a). Salt decreases the electrostatic repulsion between the particles enabling a higher seed deposition density.[11] UV-Vis spectroscopy confirms the increased density, showing a stronger extinction resulting from a larger number of gold seeds in the sample, the silica particle concentrations being equal (Figure 1b). Half of these batches were used to grow a nanoshell and the two other halves were then functionalised a second time, following the protocol described in a paper reporting a seed coverage increase from 30 to 60%.[10] In this step, pre-polymerized APTMS is used as a linker to reactivate the first gold-seeded silica core. The seed deposition was then performed without NaCl (sample A_2, synthesised from A_1) or with a salt concentration of 60 mM (sample B_2, synthesised from B_1). We observe that the UV-Vis spectrum of A_2 and B_1 are nearly overlaid meaning that the seed density is very close in both samples (Figure 1b). It demonstrates that performing a double functionalisation/deposition step is roughly equivalent to a single deposition using 60 mM NaCl in terms of achieved seed density. However, the highest density is obtained for the sample that had both treatments: double functionalisation/deposition and salt used during the deposition, as confirmed by UV-Vis and TEM images (Figures 1b-c and S1). In the electron microscopy images, the seed density difference is especially visible on the edge of particles, where we can observe individual isolated seeds for the sample with the lowest density, and a tight seed packing for the sample with the highest density. However, given the low contrast between the seeds and the silica, and the intensity change between different electron microscopy images, it is extremely difficult to provide a precise seed coverage for all the samples. We estimate coverage to be around 30-40 % for A1, 50-60% for A2 and B1, and 60-70 % for B2,

based on zoomed-in dark field TEM images (Figures 1c and S1) as performed in previous reports.[10,26]

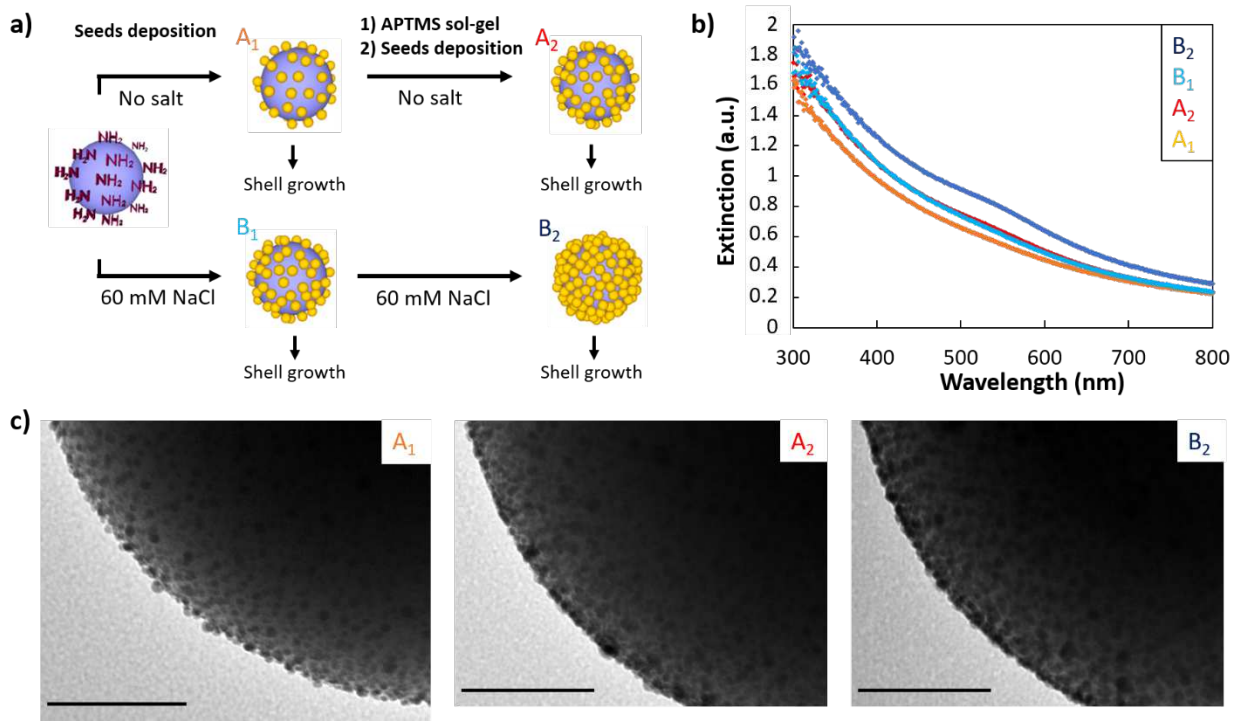

Figure 1. Silica particles covered with different gold seed densities. a) Scheme of the different parameters used during the seed deposition onto APTMS-functionalised silica particles. The four samples produced are then used to grow core@shell particles. b) UV-Vis spectroscopy of the four different seed-covered silica particle samples. c) TEM images of the samples corresponding to the three different extinction curves. Scale bars represent 50 nm.

Nanoshell synthesis

To study the effect of the seed density on the synthesis of ultrathin shells, the four previous samples, which have the same silica particle concentration and different seed densities, were used to grow a metallic shell using a gold plating solution and formaldehyde as a reducing agent. The nanoshell synthesis was performed using aliquots of the four samples of seed-covered

particles, which were mixed with different quantities of gold plating solution (100, 800, 1600 and 2666 μL, corresponding to gold salt concentrations of 0.02, 0.16, 0.32 and 0.53 mM, respectively). The optical properties of the different particles produced were measured by UV-Vis spectroscopy (Figure 2a-d). For the lowest gold plating solution volume, we observe a single peak around 520 nm, corresponding to the plasmon resonance of small gold particles. This peak strongly red shifts and intensifies with increasing gold concentration, resulting from both the particle size increase and the plasmon coupling between neighbouring gold particles.[12] This intermediate state corresponds to the formation of gold droplets on the silica surface particles, resembling raspberry-like particles (as schematised in Figure 3d),[7,8,12,13] instead of a uniform growth of seeds. The origin of this uneven particle growth is not completely clear as several phenomena might occur. Steric hindrance could explain this behaviour: the largest surface-bound seeds probably grow faster, as they have a larger reactive surface protruding farther out of the silica surface. As they grow, it becomes even more difficult for small seeds on the surface to react, therefore favouring the continuous and selective growth of the large particles, which eventually dewet to minimize surface energy. Alternatively, Preston *et al*. noted that some areas initially containing small seeds were later bare,[12] indicating that droplets are formed from several seeds. This decrease in the number of seeds could also result from particle detachment during the regrowth, observed, for example, when using very fresh gold seeds or from seeds not covalently bound to the silica surface.[27] It could also result from the increase of the attractive Van der Waals forces between neighbouring seeds during the seeds growth, forcing some of them to detach to form aggregates. Overall, this behaviour results from various mechanisms and prevents the formation of ultrathin shells. Particles produced with the highest gold plating solution volumes exhibit an increase in extinction in the near-infrared region, corresponding to droplets merging

and forming a percolated shell. High-resolution TEM images of the largest particles show a shell of approximately 12 nm on average, mostly continuous but not smooth and exhibiting faults, as evidence of the large droplet formation mechanism (Figures 2e and S2). The shape of the extinction spectra is quite typical[10,12] and differs from numerical simulations which exhibit well-defined peaks of smaller width. The difference might result from roughness and discontinuities in the metallic shell[11,2813,22] leading to a red shift and broadened resonance.[29] Good correlation between the numerical simulations of the particle extinction and the measured UV-Vis spectrum is obtained for large shell thickness (>20 nm) as the defect contribution to the optical response diminishes.[30]

Surprisingly, particles made from different seed densities possess very similar optical properties after shell growth (Figure 2a-d). Because of the strong dependence of the optical properties of nanoshells on the shell thickness,[7] this means that all samples are nearly identical. In other words, it demonstrates that the relationship between the seed density and the achievable shell thickness is more complex than originally thought. The decrease of the shell thickness reaches a plateau when the seed density is higher than 30-40% (value estimated for the sample A_1 made in a single deposition step and no salt[10,26]). We assume that this behaviour originates from the formation of the droplets, which must be relatively insensitive to the seed density above a certain threshold. This lack of effect from seed density is different to what was observed in previous papers,[10,11] however, it could be accounted for by other parameters. In Zhang and coworkers' paper,[10] the use of CO as reducing agent may produce a different formation mechanism, thus seed coverage density may impact shell thickness with this reducing agent. In García-Soto and coworker's article,[11] differences with our protocol regarding a longer seed

deposition process and the seeded-silica particle ageing, could perhaps explain the behavioural difference. We thus pursued alternative methods to decrease shell thickness.

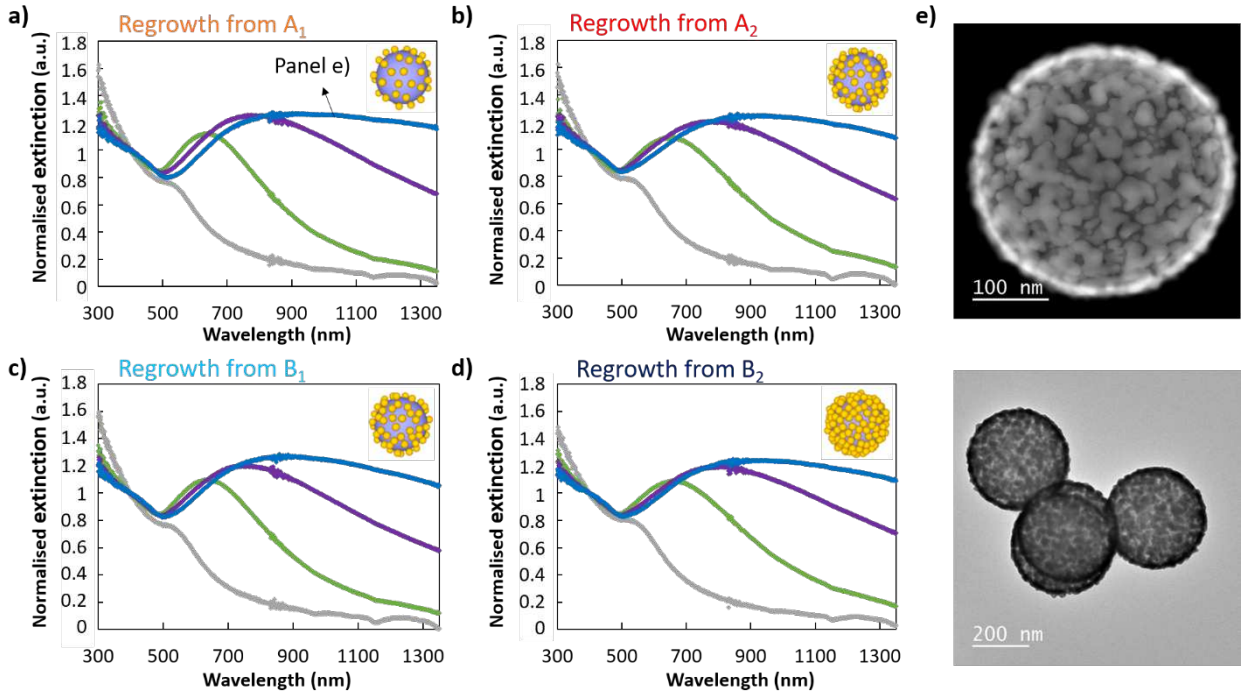

Figure 2. Core@shell optical properties. UV-Vis spectroscopy of the silica particle samples – (a) A_1, (b) A_2, (c) B_1 and (d) B_2 - after re-growth of the gold seeds with four identical gold plating solution quantities, namely a concentration of 0.02 (grey), 0.16 (green), 0.32 (purple) and 0.53 (blue) mM. e) (Top) Bright-field and (bottom) high-angle annular dark-field (HAADF) STEM images of the sample shown in blue plot in panel (a).

Comparison of the shell formation mechanism using polyvinylpyrrolidone

Based on our previous conclusions, our aim was to find an approach that minimises the formation of large gold droplets during the nanoshell synthesis, in order to achieve an ultrathin shell. It has been shown that the use of polymers, polyvinylpyrrolidone (PVP) or polyethylenimine, could affect the quality and shell thickness in the synthesis of silver

nanoshells.[23,31] For example, polyethylenimine was used as shell growth facilitator and reaction-rate regulators, favouring the formation of a thin and continuous silver shell of about 10 nm.[23] Here, we investigated this strategy and studied the effect of polyvinylpyrrolidone (PVP) on the growth of gold nanoshells. PVP is one the most widely used steric agents and exhibits a good affinity for gold as well as silica due to its amphiphilic character. When mixed to core-shell particles, it adsorbs onto the particles and form a layer whose density and thickness depend on the polymer molecular weight.[31–33] In our experiment, PVP (40 kg/mol) was added to our seeded silica particles (sample B_1) before the regrowth of the seeds. The thickness of PVP layer of such length is difficult to estimate, likely below 10 nm. Upon addition of PVP to the solution, the gold regrowth reaction rate is strongly affected, with a reaction time increasing from a few minutes to a couple of hours.

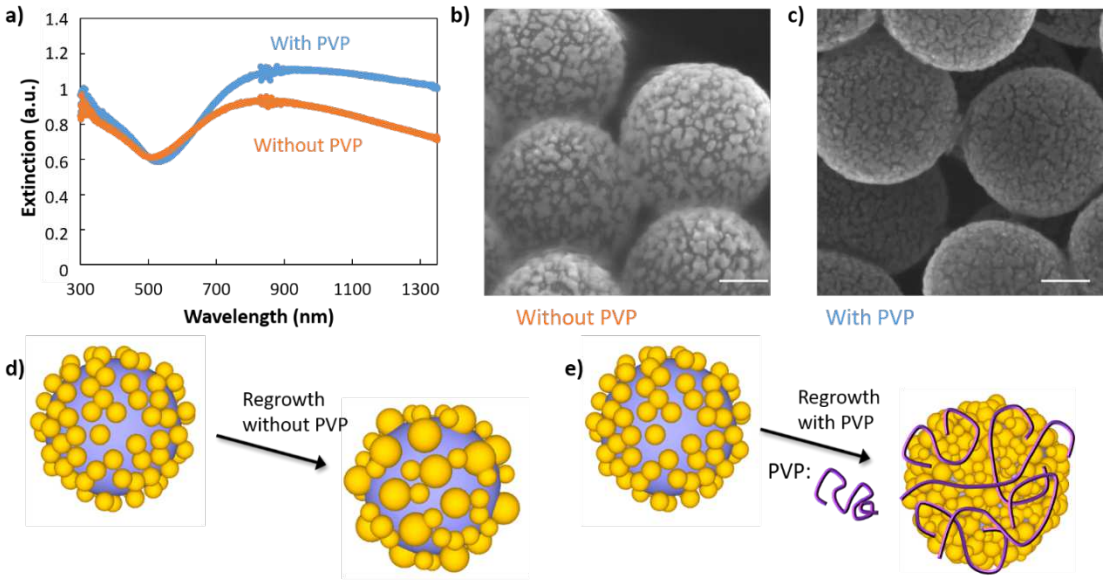

Figure 3. PVP effect on the synthesis of thin shells. a) UV-Vis spectroscopy and SEM images of core@shell particles synthesised (b) without and (c) with PVP. The scale represents 100 nm. Synthetic representation of gold nanoshell formation when the regrowth of Au seeds is performed (d) without and (e) with PVP.

The effect of PVP on the synthesis of thin nanoshells was studied by simultaneously preparing two samples, one with and one without PVP. UV-Vis spectroscopy of the samples shows that the extinction in the near-infrared region is larger for the sample prepared with PVP (Figure 3a). We also observe that the amplitude and the slope of the peak are large in the region from 500 to 800 nm, and that amplitude is higher in the near-infrared region, suggesting a more complete shell. SEM images of the two samples confirm the effect of PVP on the formation mechanism of the shell described above (Figures 3b-c). The particles prepared using PVP exhibit a higher surface coverage of gold. The gold is better distributed over the silica surface, resulting in a thinner and percolated shell (Figure 3e), thus confirming the use of polymers as a powerful tool for the fabrication of thin nanoshells. On the contrary, nanoshells prepared without PVP exhibit isolated droplets on the silica surface. A shadowing effect in this microscopy image attests to sample charging, further evidence of a non-percolating shell.

To investigate the mechanism of the shell formation with PVP, we studied the particles at intermediate stages during the shell growth. The optical extinction of the particles during shell formation, in the presence of PVP, have a gradual appearance of a broad peak in the visible upon gold regrowth (Figure 4a). The peaks are narrower and slightly blue-shifted compared to particles prepared without PVP and the same gold quantity (samples 2-3 in Figure 4a compared to green and purple curves of Figure 2b). The high-resolution TEM images show that the shell growth, in the presence of PVP, forms first numerous tiny gold islands (sample 2 in Figure 4 and Figure S3-5) which grow and merge into larger and thin patches (sample 3 in Figure 4). At this stage, the shell thickness is approximately 7 nm. The shell is continuous as shown in the insert of the Figure 4d. Overall, it is clear that PVP favours a uniform growth of the seeds and largely prevents dewetting. There are several possible explanations for the improved metal shell. First,

as previously suggested, a slower shell growth offers the possibility of matching the reaction rate and the mixing to obtain a uniform shell growth, and therefore a thinner shell.[23,31] The origin of the reaction rate being slowed down may come from interactions between Au ions and the polymer that form complexes. Also, the adsorbed PVP shell around the silica-gold core@shell likely diminishes the diffusion rate of gold ions compared to bare particles. It is also possible that the PVP shell surrounding the particles favours the gold regrowth parallel to the silica surface. Not only PVP increases the colloidal stability of the core@shell particles, it may also sufficiently shield the attracting van der Waals forces between the growing seeds, preventing the formation of clusters observed in raspberry-like nanostructures. Overall, PVP plays an important role during the growth process, improving both the smoothness and homogeneity of the obtained shells. The approach presented here opens a simple way to obtain ultra-thin metal-coated silica colloids.

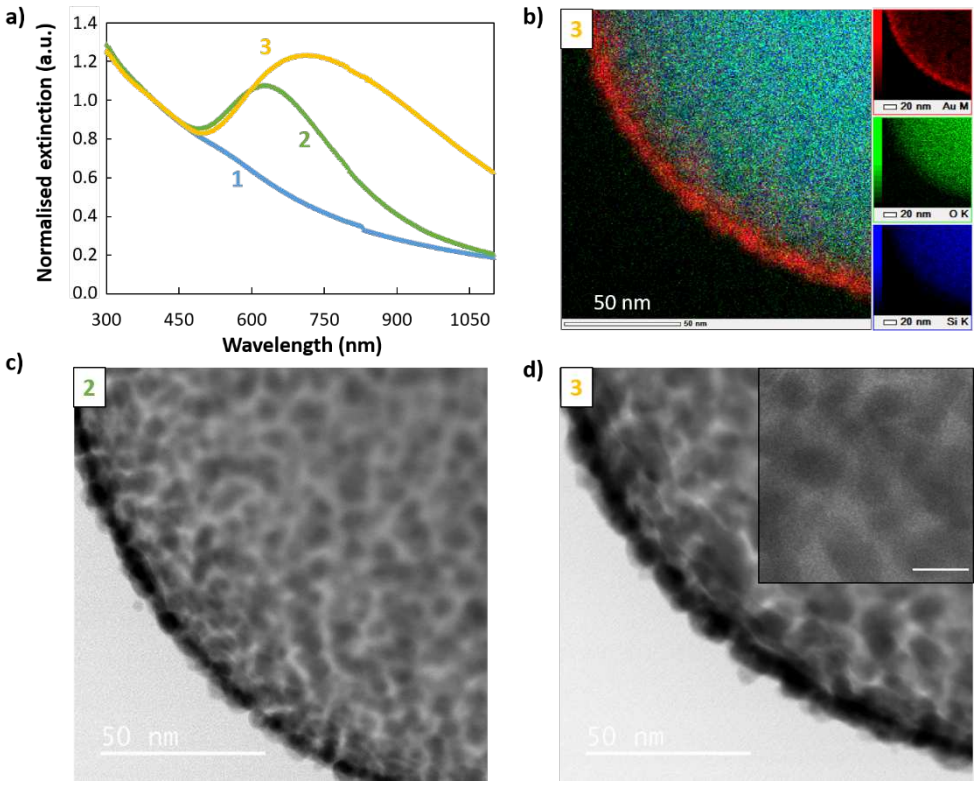

Figure 4. Characterisation of the gold shell growth synthesised in the presence of PVP. a) UV-Vis spectroscopy of seed-deposited silica particles (1) before and (2 and 3) after regrowth of the gold seeds. 2 and 3 are regrown from 1 using two different gold salt concentrations. b) STEM-EDX elemental analysis revealing (bottom right) silicon, (middle right) oxygen, (top right) gold, and (left) overlaid view of the core@shell sample 3. c-d) HAADF STEM high magnification images of samples (c) 2 and (d) 3. Inset scale bar represents 10 nm.

Post-synthesis microwave treatment

Another approach to obtain a percolating shell consists of smoothing the nanoshell post-synthesis. To do so, we performed a thermal treatment of gold nanoshells (regrown from A_2 without PVP) using microwaves. It simply consisted of a flash treatment, at 140°C, for 1 minute. Under other parameters (different microwave power and internal pressure), particle dewetting was observed (results not shown). Using these optimised conditions, improved optical properties were quickly and easily obtained. The UV-Vis spectroscopy shows that the treatment leads to a moderate increase in the extinction in the near-infrared region (Figure 5a). This is consistent with small gold islands merging into larger and smoother patches, forming a more continuous shell (Figures 5b, c, d and S6). The nature of the effect of microwaves in this process is still unclear, as the interaction between the chemicals and strong electromagnetic field is complex and because several physical parameters are modified simultaneously: localised pressure and temperature and global temperature. However, under appropriate settings, the temperature increase of the sample may occur so that the gold droplets soften without dewetting, leading to a non-quite melted, smoother and thinner, shell. It is also possible that the pressure in the vessel slows down the dewetting, compared to classical heating, offering the possibility of melting the shell before dewetting.

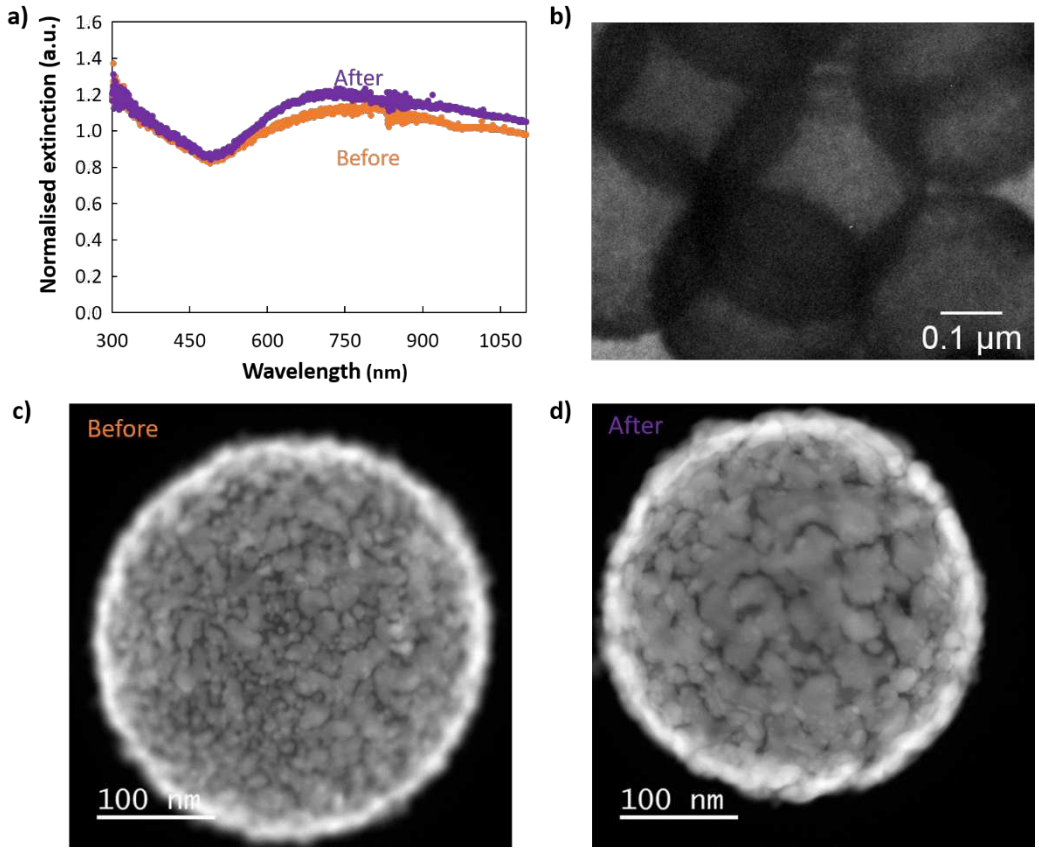

Figure 5. Flash microwave treatment of Au core@shell. (a) UV-Vis spectroscopy and HAADF STEM images of core@shell particles (c) before and (b-d) after a microwave treatment for 1 min at 140 °C.

CONCLUSIONS

Although the first synthesis of metallic nanoshells appeared 20 years ago, the synthesis of ultrathin shells with interesting extinction in the near-infrared remains challenging. We show that by combining a high ionic strength during the seed deposition with a double functionalisation/deposition step, we obtain a very high seed density on silica particles. However, we demonstrate that an increased seed density does not yield thinner shells, which we explain using the synthesis mechanism. In fact, seed regrowth is associated with the formation of

less numerous, but larger droplets and their following regrowth eventually produces inhomogeneous nanoshells whose thickness is larger than 15 nm on average.

Once establishing that the limiting factor in obtaining ultrathin shells is not the seed-deposition, but the regrowth step, we turned our attention to this process. To achieve a more homogeneous seed regrowth, PVP was added prior to the gold plating solution. This widely used steric stabilising agent prevented seeds dewetting into thicker shells, allowing a much more homogeneous coverage of smaller particles. We also employed a post-synthetic microwave treatment of the nanoshells to smooth the surface of the metallic shell. By using a flash treatment, gold particle melting, which would inevitably lead to dewetting, was avoided, successfully producing a percolated shell. The combined modifications maintained precise control over morphology and our findings could also be extended to other metals to help improve the synthesis of ultrathin Ag or Cu nanoshells of high interest for energy saving applications.

METHODS

Materials.

L-arginine (Sigma-Aldrich, 98.5%), tetraethoxysilane (TEOS, Sigma-Aldrich, 99%), ammonium hydroxide (NH_4OH, J. T. Baker, 28–30% in water), sodium hydroxide (NaOH, Sigma-Aldrich, 98%), (3-aminopropyl)trimethoxysilane (APTMS, Sigma-Aldrich, 97%), sodium chloride (NaCl, Sigma-Aldrich, ≥99.0%), gold(III) chloride trihydrate ($HAuCl_4.3H_2O$, Sigma-Aldrich, 99.9%), polyvinylpyrrolidone (PVP, MW 44,000, Sigma-Aldrich, 98%), hydrochloric acid (HCl, Sigma-Aldrich, 37%), potassium carbonate (K_2CO_3, Alfa Aesar, 95%), ethanol (Sigma-Aldrich, 99%), formaldehyde (HCHO, Sigma-Aldrich, 37 wt. % in H_2O, contains 10-

15% methanol as stabilizer) and tetrakis(hydroxymethyl)phosphonium chloride (THPC, Sigma-Aldrich, 80%) were used as received.

Synthesis.

a) Silica particles.

Silica particles were synthesised following the step-by-step published protocol.[19]

Synthesis of the silica seeds. An L-arginine aqueous solution (6 mM, 100 mL) was placed in a 150 mL double-walled vial, equipped with a reflux condenser. When the temperature stabilised at 60 °C, 10 mL of TEOS was added. The heating/stirring system was stopped when the TEOS upper phase disappeared.

First regrowth of the silica seeds. Ethanol (99%, 455 mL), ammonia (28%, 33 mL) and an aqueous dispersion of seeds (10 mL) were mixed and placed under stirring. TEOS (20 mL) was added to the solution with a syringe pump at the rate of 0.5 mL/h. Once finished, another 20 mL of TEOS was added using the same protocol. The as-obtained silica particles were approximately 125 nm in diameter. They were washed by two cycles of centrifugation/redispersion in ethanol (9,000 g, 10 min, 55 mL).

Second regrowth of the silica seeds. Ethanol (99%, 450 mL), ammonia (28%, 34 mL), water (10 mL) and the previous silica seed dispersion (5 mL) were added and stirred. Successively 20 mL, 15 mL and 8 mL of TEOS were added to the solution with a syringe pump at the rate of 0.5 mL/h. The synthesised particles were approximately 320 nm in diameter. They were purified by three cycles of centrifugation redispersion in ethanol (8,000 g, 10 min, 55 mL). The final volume of the silica nanoparticle dispersion was increased to 250 mL with ethanol and the silica concentration was measured to be 58.45 mg/mL by the dried extracts method.

b) Surface amination of the silica particles.

The previous silica particle dispersion (8.55 mL corresponding to 0.5 g) was diluted in 200 mL of ethanol. APTMS (5 mL) was added to the mixture and stirred overnight. The dispersion was then heated to reflux overnight. The aminated silica nanoparticles were purified by three cycles of centrifugation/redispersion in ethanol (8,000 g, 10 min, 25 mL). Upon the final cycle, the particles were dispersed in 40 mL of ethanol with a final measured silica concentration of 19.5 mg/mL.

c) Gold seed deposition on the silica particle surface.

Synthesis of gold seeds according to the Duff's protocol.[34] Water (227.5 mL) was mixed with 0.2 M NaOH (7.5 mL) and 5 mL of diluted THPC (120 µL of the stock solution diluted in 10 mL of water) for 15 min. Then, 5 mL of $HAuCl_4$ (25 mM) was quickly added and the solution changed from colourless to brown immediately, indicating the formation of gold seeds. The as-prepared gold-seed solution was kept at 4°C for 14 days before use.

First deposition of the gold seeds onto the silica core (samples A_1 and B_1). APTMS-functionalised silica nanoparticles (1.5 mL) were added to 38.5 mL of gold seed solution without NaCl (A_1) or with an additional 3.478 mL of 1 M NaCl (B_1). The dispersions were slowly agitated overnight. Excess gold seeds were removed by two cycles of centrifugation/redispersion in water (6000 g, 10 min, 40 mL). After the final cycles, the particles were redispersed in water (10 mL).

Preparation of pre-polymerized APTMS solution. This synthesis was adapted from a published protocol.[10] Two volumes of 33 mL of water were mixed with 1.11 mL of HCl (0.1 M) and 1.33 mL of APTMS (stock solution) and vigorously stirred for 1h.

Second deposition of the gold seeds onto the silica core (samples A_2 and B_2). The two dispersions of gold-seeded silica cores (5 mL, samples A_1 and B_1) were mixed with the pre-

polymerized APTMS solution (35.44 mL each) and stirred for 20 min. Then excess pre-polymerized APTMS was removed by three cycles of centrifugation/redispersion in water (6000 g, 10 min, 40 mL). After the final cycle, the particles were redispersed in 20 mL of gold-seed solution without NaCl (sample A_2) or with an additional 1.739 mL of 1 M NaCl (sample B_2). The dispersions were slowly stirred overnight. The excess of gold seeds was removed by two cycles of centrifugation/redispersion in water (6000 g, 10 min, 40 mL). After the final cycle, the particles were redispersed in water (5 mL).

d) Formation of the thin metallic shell by a controlled gold seed growth.

Preparation of the gold plating solution. 50 mL of an aqueous solution containing 4 mL of $HAuCl_4$ (25 mM) and 125 mg of K_2CO_3 were prepared and stirred for 3 h. A colour change from yellow to colourless was observed. The gold plating solution was stored in the dark at 4 °C for 24 h.

Gold seed growth. The gold-seeded silica particles (250 μL, A_1, A_2, B_1 and B_2) were mixed with water and with different volumes of gold plating solution and formaldehyde. Water was first added so that the final volume of the solution was 10 mL. For the experiments displayed in Figure 2a-d, the gold plating solution volumes used were 100, 800, 1600, and 2666 μL, respectively. The volume of formaldehyde added was 1/20 of the gold plating solution volume, with a maximum of 40 μL of formaldehyde. The colour change occurred within a few minutes. The excess reactants were removed by two cycles of centrifugation/redispersion in water (from 1000 to 4000 g depending on shell thickness, 5 min, 10 mL). After the final cycles, the particles were redispersed in water (10 mL).

Gold seed growth in presence of polyvinylpyrrolidone. The previous protocol was carried out except that aqueous solution of PVP (1 mL, 10 g/L) was added before the gold plating solution.

The colour change occurred over a few hours instead of minutes. After the final centrifugation, the solutions were redispersed in PVP solution (10 mL, 1 g/L).

e) Microwave treatment.

An Anton Paar microwave reactor (Monowave 450) equipped with an autosampler (MAS 24) was used. The as-synthesised particles (2 mL), regrown from A_2 without PVP, were added to water (18 mL) in a 30 mL vial. The solution was heated with microwave radiation to 140 °C for 1 min.

Characterisation

a) Electron microscopy characterisation.

Scanning transmission electron microscopy (STEM) studies were performed using a JEOL cold-FEG JEM-ARM200F operating at 200 kV equipped with a probe Cs corrector reaching a spatial resolution of 0.078 nm. EDX spectra were recorded on a JEOL CENTURIO SDD detector. For Transmission electron microscopy (TEM) experiments, samples were prepared by depositing one drop of the colloidal dispersion onto a conventional carbon-coated copper grid. Grids were air dried at room temperature and stored in a closed box to prevent dust accumulating. TEM experiments were performed using a JEOL JEM 1400+ operating at 120 kV with a LaB6 filament. Scanning electron microscopy (SEM) experiments were performed on a SEM-FEG HR - JEOL 6700F.

b) Optical characterisation.

UV-Vis spectroscopy spectra were recorded on a Shimadzu UV-3600 UV-VIS-NIR.

ASSOCIATED CONTENT

Supporting Information. The section contains supplementary TEM and HTREM images of the core@shell particles synthesised, with or without, PVP and using a microwave treatment.

REFERENCES

1. Neumann, O. *et al*. Solar Vapor Generation Enabled by Nanoparticles. *ACS Nano* **7**, 42–49 (2013).
2. Bardhan, R., Grady, N. K., Cole, J. R., Joshi, A. & Halas, N. J. Fluorescence Enhancement by Au Nanostructures: Nanoshells and Nanorods. *ACS Nano* **3**, 744–752 (2009).
3. Jiang, Q. *et al*. Enhanced performance of dye-sensitized solar cells using silica/gold core–shell spheres modified photoanodes. *Mater. Lett.* **134**, 16–19 (2014).
4. Khlebtsov, B. N. & Khlebtsov, N. G. Biosensing potential of silica/gold nanoshells: Sensitivity of plasmon resonance to the local dielectric environment. *J. Quant. Spectrosc. Radiat. Transf.* **106**, 154–169 (2007).
5. Brongersma, M. L. Nanoshells: gifts in a gold wrapper. *Nat. Mater.* **2**, 296–297 (2003).
6. Bardhan, R., Lal, S., Joshi, A. & Halas, N. J. Theranostic Nanoshells: From Probe Design to Imaging and Treatment of Cancer. *Acc. Chem. Res.* **44**, 936–946 (2011).
7. Oldenburg, S. J., Averitt, R. D., Westcott, S. L. & Halas, N. J. Nanoengineering of optical resonances. *Chem. Phys. Lett.* **288**, 243–247 (1998).
8. Yong, K.-T., Sahoo, Y., Swihart, M. T. & Prasad, P. N. Synthesis and plasmonic properties of silver and gold nanoshells on polystyrene cores of different size and of gold–silver core–shell nanostructures. *Colloids Surf., A* **290**, 89–105 (2006).
9. Brinson, B. E. *et al*. Nanoshells Made Easy: Improving Au Layer Growth on Nanoparticle Surfaces. *Langmuir* **24**, 14166–14171 (2008).

10. Zhang, X. *et al*. Metallic Nanoshells with Sub-10 nm Thickness and Their Performance as Surface-Enhanced Spectroscopy Substrate. *ACS Appl. Mater. Interfaces* **8**, 9889–9896 (2016).

11. García-Soto, M. J. & González-Ortega, O. Synthesis of silica-core gold nanoshells and some modifications/variations. *Gold Bull* **49**, 111–131 (2016).

12. Preston, T. C. & Signorell, R. Growth and Optical Properties of Gold Nanoshells Prior to the Formation of a Continuous Metallic Layer. *ACS Nano* **3**, 3696–3706 (2009).

13. Brito-Silva, A. M. *et al*. Improved Synthesis of Gold and Silver Nanoshells. *Langmuir* **29**, 4366–4372 (2013).

14. Lim, Y. T., Park, O. O. & Jung, H.-T. Gold nanolayer-encapsulated silica particles synthesized by surface seeding and shell growing method: near infrared responsive materials. *J. Colloid Interface Sci*. **263**, 449–453 (2003).

15. Jankiewicz, B. J., Jamiola, D., Choma, J. & Jaroniec, M. Silica–metal core–shell nanostructures. *Adv. Colloid Interface Sci*. **170**, 28–47 (2012).

16. Phonthammachai, N. *et al*. Synthesis of Contiguous Silica−Gold Core−Shell Structures: Critical Parameters and Processes. *Langmuir* **24**, 5109–5112 (2008).

17. Kah, J. C. Y. *et al*. Synthesis of gold nanoshells based on the depositionprecipitation process. *Gold Bull* **41**, 23–36 (2008).

18. Saini, A. *et al*. Synthesis and SERS Application of SiO2@Au Nanoparticles. *Plasmonics* **10**, 791–796 (2015).

19. Park, S., Park, M., Han, P. & Lee, S. Relative Contributions of Experimental Parameters to NIR-Absorption Spectra of Gold Nanoshells. *J. Ind. Eng. Chem*. **13**, 65–70 (2007).

20. Dement'eva, O. V., Kartseva, M. E., Sukhov, V. M. & Rudoy, V. M. Evolution of ultrafine gold seed nanoparticles with temperature and time and synthesis of plasmonic nanoshells. *Colloid J* **79**, 605–610 (2017).

21. Liu, S. *et al*. A Facile Approach to the Synthesis of Gold Nanoshells with Near Infrared Responsive Properties. *Chin. J. Chem.* **27**, 1079–1085 (2009).

22. Liang, Z. *et al*. The effect of pH value on the formation of gold nanoshells. *J Nanopart Res* **13**, 3301–3311 (2011).

23. Maw, S. S., Watanabe, S. & Miyahara, M. T. Multiple Roles of Polyethylenimine during Synthesis of 10 nm Thick Continuous Silver Nanoshells. *Langmuir* **36**, 4511–4518 (2020).

24. Hartlen, K. D., Athanasopoulos, A. P. T. & Kitaev, V. Facile Preparation of Highly Monodisperse Small Silica Spheres (15 to >200 nm) Suitable for Colloidal Templating and Formation of Ordered Arrays. *Langmuir* **24**, 1714–1720 (2008).

25. Westcott, S. L., Jackson, J. B., Radloff, C. & Halas, N. J. Relative contributions to the plasmon line shape of metal nanoshells. *Phys. Rev. B* **66**, 155431 (2002).

26. Radloff, C. J. Concentric nanoshells and plasmon hybridization. (2004).

27. Oldenburg, S. J. Light scattering from gold nanoshells. (2000).

28. Sun, H. *et al*. Silica–Gold Core–Shell Nanosphere for Ultrafast Dynamic Nanothermometer. *Adv. Funct. Mater.* **24**, 2389–2395 (2014).

29. Wang, H. *et al*. Controlled Texturing Modifies the Surface Topography and Plasmonic Properties of Au Nanoshells. *J. Phys. Chem. B* **109**, 11083–11087 (2005).

30. Oldenburg, S. J., Jackson, J. B., Westcott, S. L. & Halas, N. J. Infrared extinction properties of gold nanoshells. *Appl. Phys. Lett.* **75**, 2897–2899 (1999).

31. Maw, S. S., Watanabe, S. & Miyahara, M. T. Flow synthesis of silver nanoshells using a microreactor. *Chem. Eng. J.* **374**, 674–683 (2019).

32. Tsuji, M. *et al*. Effects of chain length of polyvinylpyrrolidone for the synthesis of silver nanostructures by a microwave-polyol method. *Mater. Lett.* **60**, 834–838 (2006).

33. Haesuwannakij, S. *et al*. The Impact of the Polymer Chain Length on the Catalytic Activity of Poly(N -vinyl-2-pyrrolidone)-supported Gold Nanoclusters. *Sci. Rep.* **7**, 9579 (2017).

34. Duff, D. G., Baiker, A. & Edwards, P. P. A new hydrosol of gold clusters. 1. Formation and particle size variation. *Langmuir* **9**, 2301–2309 (1993).

ACKNOWLEDGMENTS

TEM experiments were performed at the Plateforme Aquitaine de Caractérisation des Matériaux (UAR CNRS 3626) of the University of Bordeaux and at the Centre de Microcaractérisation Raimond Castaing (UAR CNRS 3623) of the University of Toulouse. We gratefully acknowledge Teresa Hungria for her assistance in mapping analysis.

AUTHOR INFORMATION

Corresponding Author

*E-mail: laurent.lermusiaux@ens-lyon.fr; mona.treguer@icmcb.cnrs.fr

Present Address of L.Lermusiaux

Laboratoire de Chimie, CNRS, Ecole Normale Supérieure de Lyon, 46 allée d'Italie, 69364 Lyon, France

Author contributions statement

LL and MP synthesised the core@shell particles. LL and GD did the electron microscopy. LB, MP and MTD supervised the particles synthesis and characterization experiments. TLM, VB, ED and MTD acquired funding for the project. LL, GD and MTD wrote the manuscript, with input and edits from all authors.

Funding Sources

This work was jointly supported by the Solvay company and the LabEx AMADEus (ANR-10-LABX-42) in the framework of IdEx Bordeaux (ANR-10-IDEX-03-02), *i.e.* the Investissements d'Avenir program of the French government managed by the Agence Nationale de la Recherche.

Competing interests

The author(s) declare no competing interests.

Figure Legends

Figure 1. Silica particles covered with different gold seed densities. a) Scheme of the different parameters used during the seed deposition onto APTMS-functionalised silica particles. The four samples produced are then used to grow core@shell particles. b) UV-Vis spectroscopy of the four different seed-covered silica particle samples. c) TEM images of the samples corresponding to the three different extinction curves. Scale bars represent 50 nm.

Figure 2. Core@shell optical properties. UV-Vis spectroscopy of the silica particle samples – (a) A_1, (b) A_2, (c) B_1 and (d) B_2 - after re-growth of the gold seeds with four identical gold plating solution quantities, namely a concentration of 0.02 (grey), 0.16 (green), 0.32 (purple) and 0.53 (blue) mM. e) (Top) Bright-field and (bottom) high-angle annular dark-field (HAADF) STEM images of the sample shown in blue plot in panel (a).

Figure 3. PVP effect on the synthesis of thin shells. a) UV-Vis spectroscopy and SEM images of core@shell particles synthesised (b) without and (c) with PVP. The scale represents 100 nm. Synthetic representation of gold nanoshell formation when the regrowth of Au seeds is performed (d) without and (e) with PVP.

Figure 4. Characterisation of the gold shell growth synthesised in the presence of PVP. a) UV-Vis spectroscopy of seed-deposited silica particles (1) before and (2 and 3) after regrowth of the gold seeds. 2 and 3 are regrown from 1 using two different gold salt concentrations. b) STEM-EDX elemental analysis revealing (bottom right) silicon, (middle right) oxygen, (top right) gold, and (left) overlaid view of the core@shell sample 3. c-d) HAADF STEM high magnification images of samples (c) 2 and (d) 3. Inset scale bar represents 10 nm.

Figure 5. Flash microwave treatment of Au core@shell. (a) UV-Vis spectroscopy and HAADF STEM images of core@shell particles (c) before and (b-d) after a microwave treatment for 1 min at 140 °C.

Figures

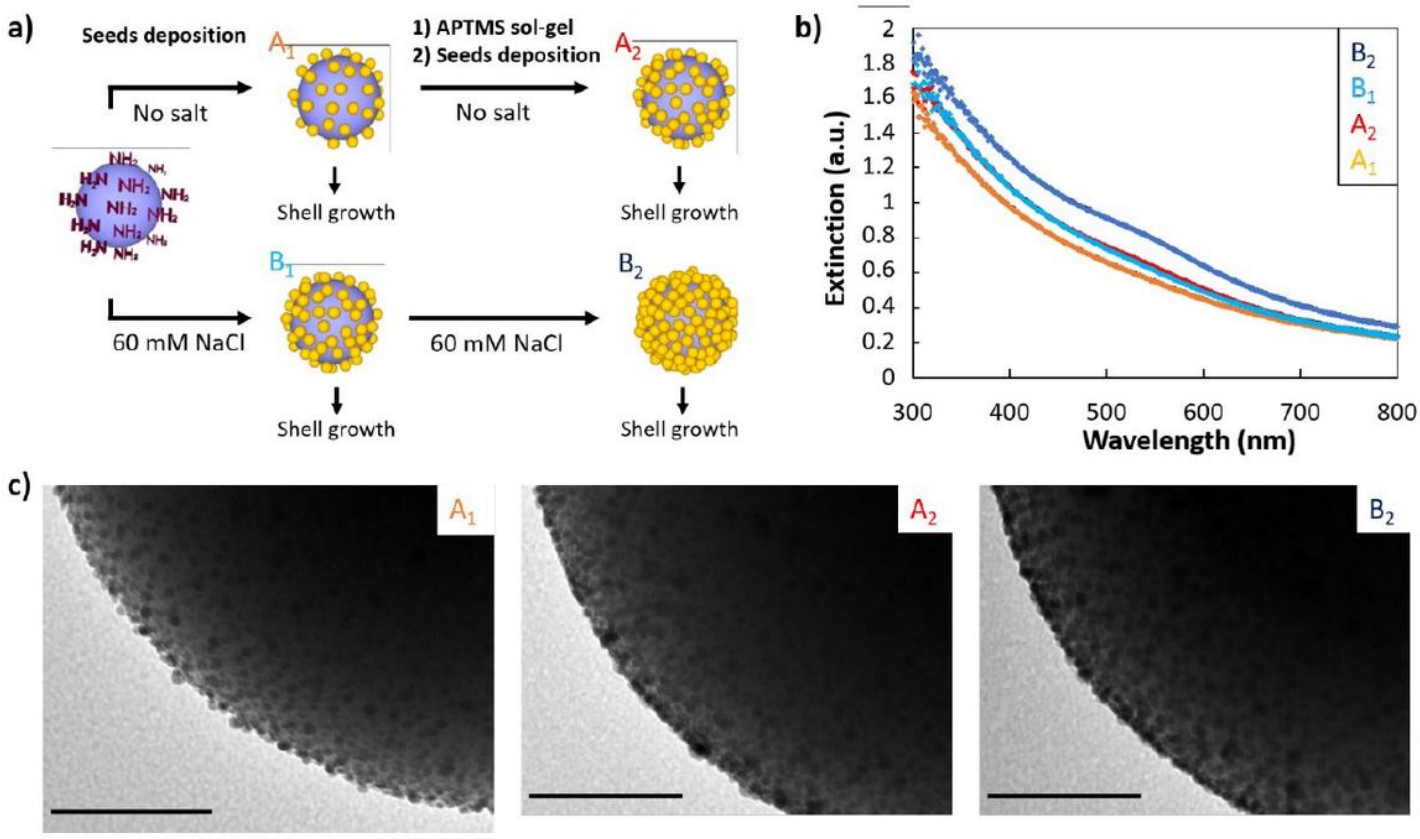

Figure 1

Silica particles covered with different gold seed densities. a) Scheme of the different parameters used during the seed deposition onto APTMS-functionalised silica particles. The four samples produced are then used to grow core@shell particles. b) UV-Vis spectroscopy of the four different seed-covered silica particle samples. c) TEM images of the samples corresponding to the three different extinction curves. Scale bars represent 50 nm.

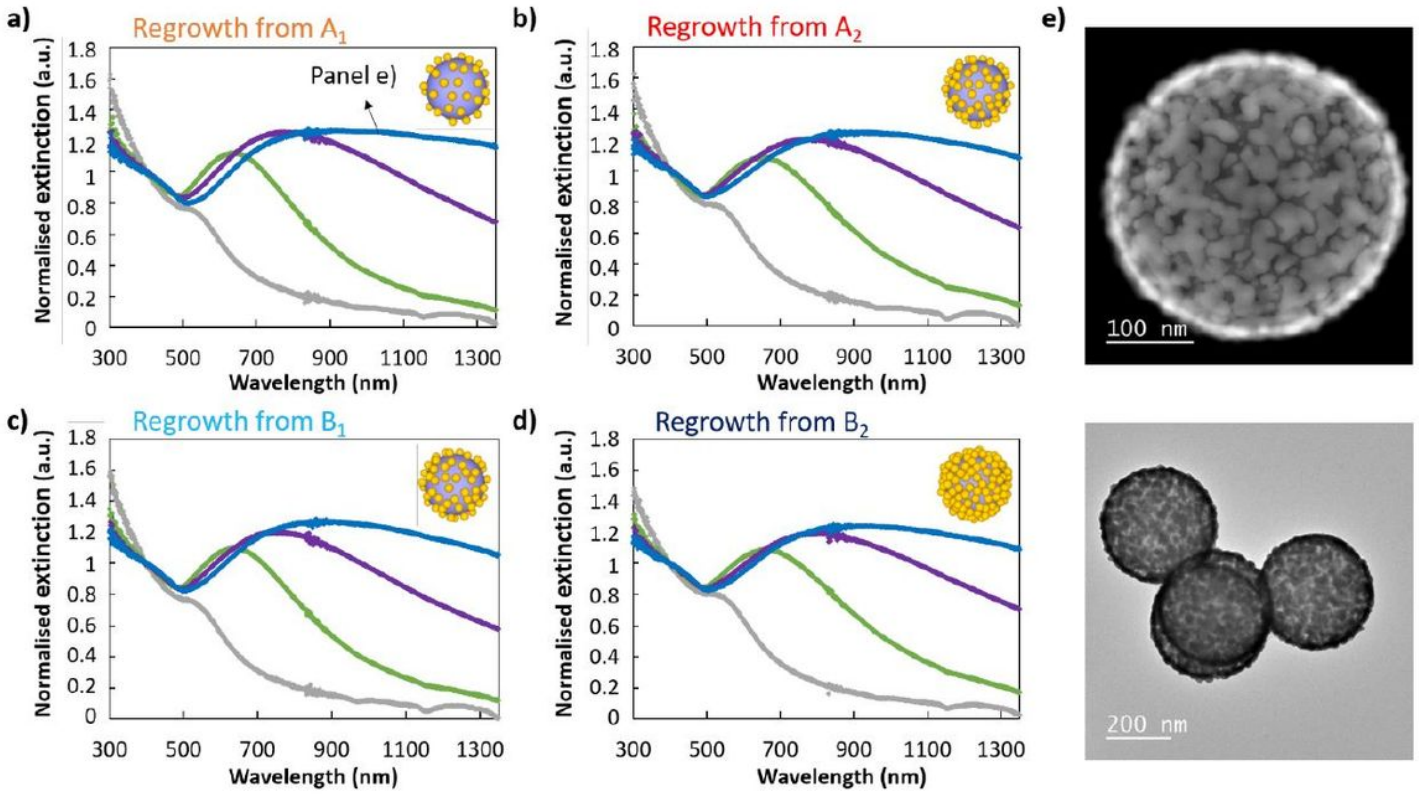

Figure 2

Core@shell optical properties. UV-Vis spectroscopy of the silica particle samples – (a) A1, (b) A2, (c) B1 and (d) B2 - after re-growth of the gold seeds with four identical gold plating solution quantities, namely a concentration of 0.02 (grey), 0.16 (green), 0.32 (purple) and 0.53 (blue) mM. e) (Top) Bright-field and (bottom) high-angle annular dark-field (HAADF) STEM images of the sample shown in blue plot in panel (a).

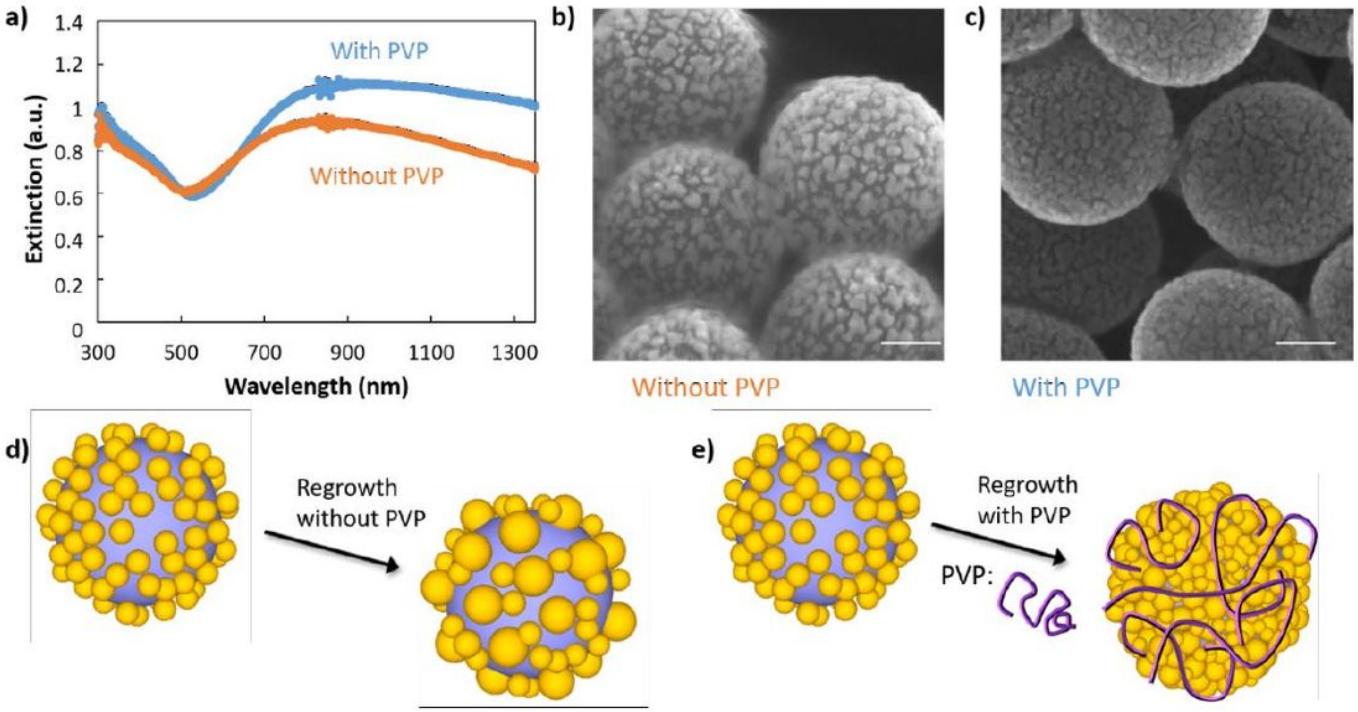

Figure 3

PVP effect on the synthesis of thin shells. a) UV-Vis spectroscopy and SEM images of core@shell particles synthesised (b) without and (c) with PVP. The scale represents 100 nm. Synthetic representation of gold nanoshell formation when the regrowth of Au seeds is performed (d) without and (e) with PVP.

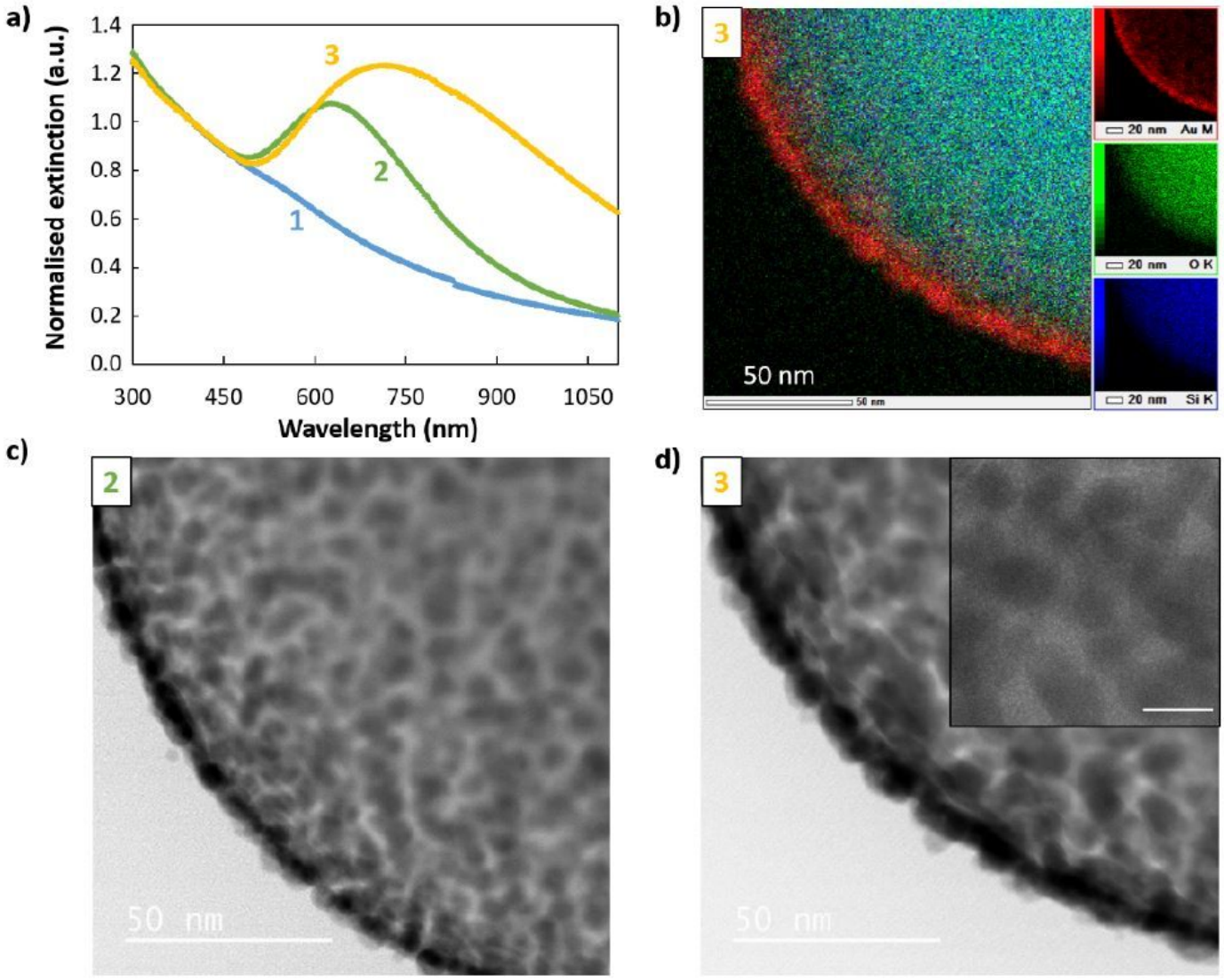

Figure 4

Characterisation of the gold shell growth synthesised in the presence of PVP. a) UVVis spectroscopy of seed-deposited silica particles (1) before and (2 and 3) after regrowth of the gold seeds. 2 and 3 are regrown from 1 using two different gold salt concentrations. b) STEMEDX elemental analysis revealing (bottom right) silicon, (middle right) oxygen, (top right) gold, and (left) overlaid view of the core@shell sample 3. c-d) HAADF STEM high magnification images of samples (c) 2 and (d) 3. Inset scale bar represents 10 nm.

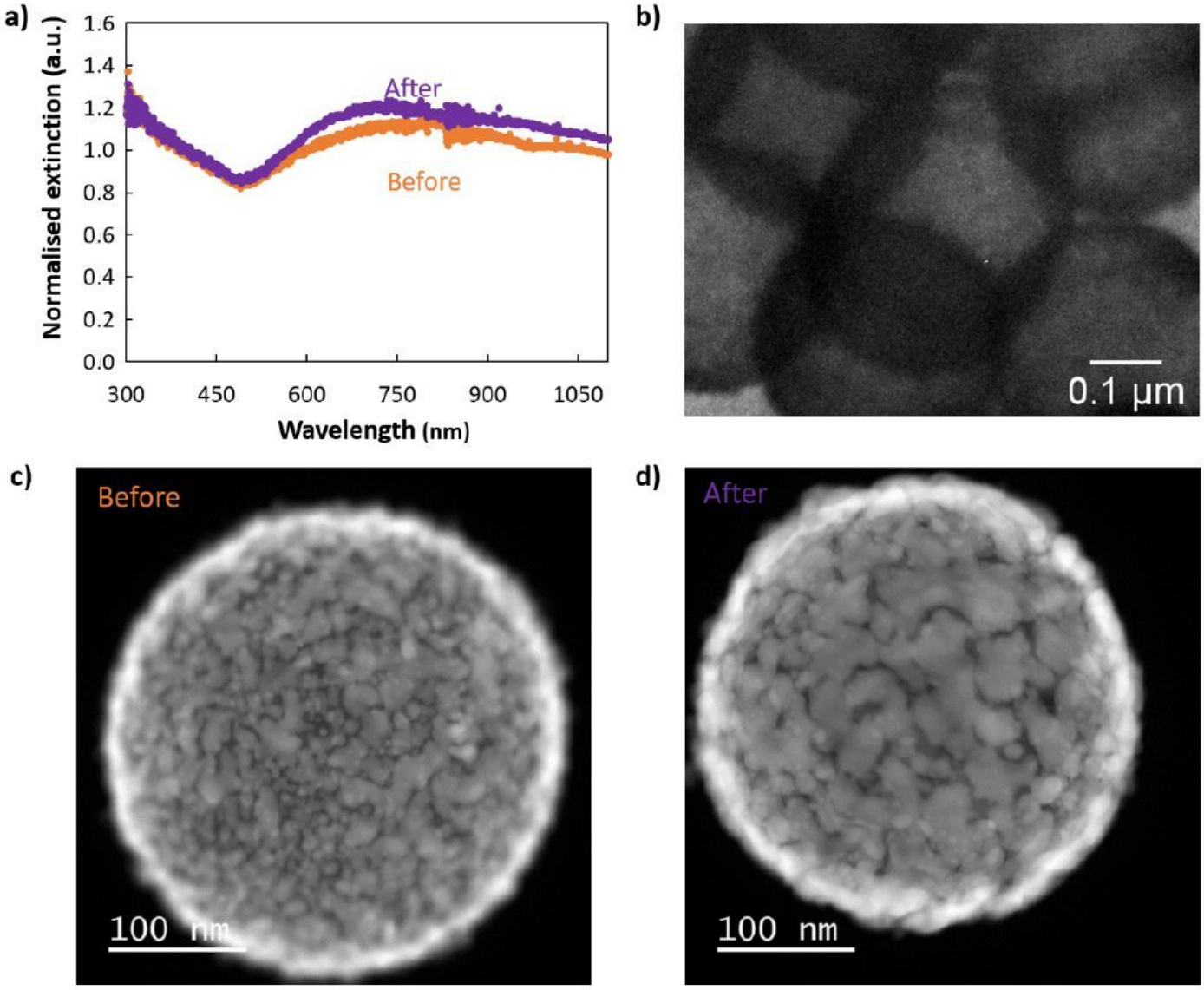

Figure 5

Flash microwave treatment of Au core@shell. (a) UV-Vis spectroscopy and HAADF STEM images of core@shell particles (c) before and (b-d) after a microwave treatment for 1 min at 140 °C.

Supplementary Files

This is a list of supplementary files associated with this preprint. Click to download.

- SILERMUSIAUX.pdf